

Ruling Out Bosonic Repulsive Dark Matter in Thermal Equilibrium

Zachary Slepian^{*} and Jeremy Goodman[†]

Department of Astrophysical Sciences, Princeton University, Princeton, NJ, 08544

17 September 2018

ABSTRACT

Self-interacting dark matter (SIDM), especially bosonic, has been considered a promising candidate to replace cold dark matter (CDM) as it resolves some of the problems associated with CDM. Here, we rule out the possibility that dark matter is a repulsive boson in thermal equilibrium. We develop the model first proposed by Goodman (2000) and derive the equation of state at finite temperature. Isothermal spherical halo models indicate a Bose-Einstein condensed core surrounded by a non-degenerate envelope, with an abrupt density drop marking the boundary between the two phases. Comparing this feature with observed rotation curves constrains the interaction strength of our model’s DM particle, and Bullet Cluster measurements constrain the scattering cross section. Both ultimately can be cast as constraints on the particle’s mass. We find these two constraints cannot be satisfied simultaneously in any realistic halo model—and hence dark matter cannot be a repulsive boson in thermal equilibrium. It is still left open that DM may be a repulsive boson provided it is not in thermal equilibrium; this requires that the mass of the particle be significantly less than a millivolt.

Key words: dark matter, galaxies: haloes, cosmology: theory, cosmology: observations

1 INTRODUCTION

There is much observational evidence for dark matter— M/L ratios in low surface brightness galaxies (LSB’s), flat rotation curves in spiral galaxies, the Oort discrepancy, gravitational lensing, cluster gas masses, the cosmic microwave background (CMB) combined with Big Bang nucleosynthesis (BBN) (Komatsu et al. 2011, Bertone et al. 2005, Sahní 2004, Peebles 1993)—but its essence remains elusive. The standard model has been cold, non-interacting dark matter (CDM), which, while successful in simulations of large-scale structure formation, is less so in the details. Steep density profiles (Colin et al. 2004) (though better baryon physics may improve this: see Cole et al. 2011 and Jardel & Sellwood 2009), overproduction of small halos (Mikheeva et al. 2007, Diemand et al. 2005), failure to predict the zero point of the Tully-Fisher relation (Mo & Mao 2000), and spiral galaxy bar rotation speeds (De Battista & Sellwood 2000, 1998) all present unresolved questions for CDM.

In the early aughts, self-interacting dark matter (SIDM) appeared appealing because it promised to resolve some of these questions. A spate of papers explored SIDM (Spergel & Steinhardt 2000, Goodman 2000, Wandelt 2000, Peebles 2000) and of late interest has returned to this topic (Loeb & Weiner 2011, Su & Chen 2011). In particular, bosonic SIDM has provoked considerable theoretical work (Chavanis 2011, Rindler-Daller & Shapiro 2011, Rindler-Daller & Shapiro 2010), especially as scalar-field dark matter (SFDM) (the scalar field encodes a self-interaction) (Briscese 2011, Amaro-Seoane et al. 2010, Lee 2009, Lee & Lim 2010, Urena-Lopez 2009, Bernal et al. 2008, Bernal & Guzman 2006, Matos & Urena-Lopez 2002). We also note that many have studied non-self-interacting bosonic dark matter; see Harko 2011 I and II, Bernal et al. 2008, and Urena-Lopez 2009. Non-bosonic self-interacting dark matter has also been considered; see Koda & Shapiro 2011, Ahn & Shapiro 2005, Mitra 2005, and Hennawi & Ostriker 2001.

Given this, it is worthwhile to consider whether SIDM could produce realistic halo density profiles and rotation curves, with the aim of moving away from these models if they cannot. In this paper, we calculate density profiles and rotation curves for a representative such model first presented in Goodman 2000. The dark matter is a short-range

^{*} E-mail: zslepian@cfa.harvard.edu

[†] E-mail: jeremy@astro.princeton.edu

repulsively interacting boson with repulsion strength, mass, and interaction cross section to be determined by observational constraints. We place an upper bound on the DM particle mass using a constraint from the Bullet Cluster, and a lower bound on the mass by demanding that the dark matter halo, modeled as an isothermal sphere, produce an observationally allowed rotation curve. Note that this second constraint applies only if the DM is in thermal equilibrium (further discussion in §5).

These two constraints are incompatible: the lower bound is greater than the upper bound. Hence we conclude that bosonic repulsive dark matter (RDM) in thermal equilibrium can be ruled out. This conclusion can be avoided if RDM halos have not reached even local thermodynamic equilibrium by the present epoch. However, in that case the model is very similar to the traditional, effectively non-interacting axion (because the scattering must be small enough so as not to produce thermal equilibrium), except that collective repulsion could still support a core. Streaming motions would be required to explain the extended parts of the halo outside the core, as with conventional noninteracting dark matter. Further discussion of these points occurs in §5.

The paper is structured as follows. In §2, we compute the scattering cross section and pressure. In §3, we present isothermal spherical halo models. In §4, we combine the constraints of §2 and §3 and show that they cannot simultaneously be satisfied. We discuss our results and conclude in §5. In two Appendices, we discuss the calculations behind the equation of state and examine the drag on a perturbation to the halo, e.g. a rotating galactic bar.

Throughout, σ denotes a cross section and m the dark matter particle's mass. ν is always a number density. We define all other symbols where they are used, and also provide a table of the main symbols defined in this paper and their meanings for easy reference (Table 1).

2 SCATTERING CROSS SECTION AND PRESSURE

2.1 Details of the RDM

As preliminary to the scattering cross section and pressure, we present an overview of the RDM model, beginning with the relativistic formalism, moving on to discuss the minimum core size, and concluding with other remarks. Like the axion, the DM particles are bosonic and are supposed to be born in a Bose-Einstein condensate (BEC) in the early universe (Goodman 2000, Peebles 2000). Peebles and Goodman both argued that if present-day repulsive dark matter derives from a relativistic scalar field, then it has acceptable behavior in the early universe, *i.e.* it does not suppress large-scale structure or unduly affect primordial nucleosynthesis.

The dark matter particles' interaction would naturally be short-range, in fact point-like, if it corresponded to the non-relativistic limit of a massive complex scalar field with mass m and a momentum-independent self-interaction term $V(\phi, \phi^*) = \lambda(\phi^* \phi)^2$. We therefore treat the RDM as an assemblage of non-relativistic point particles of mass m having a two-body interaction potential U whose range is small compared to the particles' de Broglie wavelength, so that

$U(\mathbf{x}_1 - \mathbf{x}_2) \rightarrow U_0 \delta(\mathbf{x}_1 - \mathbf{x}_2)$. The constant $U_0 \equiv \tilde{U}(0)$ is the Fourier transform of $U(\Delta \mathbf{x})$ evaluated at zero momentum.

At tree level, $U_0 = \lambda \hbar^3 / 4m^2 c$ in conventional units, λ being dimensionless and nonnegative. In contrast to Goodman (2000), we have taken the field to be complex so that the particles are conserved, being protected from mutual annihilation via this same interaction term by a global phase symmetry $\phi \rightarrow e^{i\psi} \phi$.¹ Otherwise the particles would annihilate via a cascade of stimulated emission in less than a Hubble time, unless their mass were so small and their interaction so weak as to preclude the establishment of local thermodynamic equilibrium (Riotto & Tkachev 2000).

In the condensate, pressure varies only with density. With a quartic self-interaction potential such as we have adopted above, Goodman (2000) notes that in the non-relativistic limit $P \ll \rho c^2$, pressure and density are related as in an $n = 1$ Emden polytrope, $P = K \rho^2$, with $K = U_0 / 2m^2$. The density profile is

$$\rho(r) = \rho(0) \frac{\sin(\pi r / r_c)}{\pi r / r_c} \quad (1)$$

with $0 \leq r \leq r_c$ and core radius

$$r_c = \sqrt{\frac{\pi K}{2G}} = \sqrt{\frac{\pi U_0}{4Gm^2}}. \quad (2)$$

The total mass within r_c associated with the profile (1) is $M_c = 4\rho(0)r_c^3/\pi$. The velocity v_c of a circular orbit at the edge of the core is therefore given by

$$v_c^2 \equiv \frac{GM_c}{r_c} = \frac{4G\rho(0)r_c^2}{\pi} = 2K\rho(0) = \frac{\rho(0)U_0}{m^2}, \quad (3)$$

in which the second and third equalities result from eliminating r_c^2 using eq. (2).

If all of the DM were still in the condensate, then all non-rotating dark halos in virial equilibrium would have this size and density profile independent of their masses. Clearly this would not be acceptable, especially if the core radius $r_c \sim 1$ kpc as required to match the DM cores of dwarf galaxies. However, more complex and extended profiles can be obtained if the DM has a finite temperature, as we discuss in the remainder of this paper, or where it has not yet reached thermal or even hydrostatic equilibrium.

As we will show, the scattering cross section per unit mass is $\sigma_{\text{scatt}}/m = mU_0^2/2\pi\hbar^4$. Since this involves a combination of m and U_0 independent from that appearing in the core radius (2), the degree of collisionality of RDM is independent of its minimum core size. Thus it seems possible to evade the constraint on σ_{scatt}/m set by the Bullet Cluster (Randall et al. 2008). However, as will be shown, one then encounters difficulties with halo rotation curves.

2.2 Scattering Cross Section

In the first-order Born approximation, the interaction potential $U(\mathbf{x}_1, \mathbf{x}_2) = U_0 \delta(\mathbf{x}_1 - \mathbf{x}_2)$ between identical nonrel-

¹ What is actually conserved is the (non-electromagnetic) "charge" represented by the number of particles minus the number of antiparticles. For a relativistic chemical potential $\mu = \mu_{\text{NR}} + mc^2$, with nonrelativistic counterpart μ_{NR} , in the nonrelativistic limit the antiparticles become so sparse that "charge" can be identified with particle number.

ativistic bosons entails the scattering cross section

$$\sigma_{\text{scatt}} = \frac{m^2 U_0^2}{2\pi\hbar^4}. \quad (4)$$

We can eliminate U_0 and rewrite σ_{scatt} in terms of the core radius (2):

$$\sigma_{\text{scatt}} = \frac{8G^2 m^6 r_c^4}{\pi^3 \hbar^4}. \quad (5)$$

From the Bullet Cluster, we have the constraint that $\sigma_{\text{scatt}}/m < 1.25 \text{ cm}^2 \text{ g}^{-1}$ (Randall et al. 2008); substituting eq. (5) into this relation implies that

$$m < 9.6 \times 10^{-4} \times \left(\frac{r_c}{1 \text{ kpc}} \right)^{-4/5} \text{ eV}/c^2. \quad (6)$$

We emphasize that r_c in eq. (6) is the minimum size of a halo core supported only by repulsion; a larger core radius is allowed for a given particle mass if the core is partly or entirely supported by random motions, as it must be for non-interacting DM.

Now, the Bullet Cluster bound was derived from N-body simulations of classical particles with dynamics specified completely by gravity and contact collisions. Furthermore, the initial halo density profiles before the merger were King profiles. Since the DM we consider here is bosonic, and our initial density profile does differ from the King profile, it is worth pausing to establish that Randall et al.’s bound really does apply. In both their simulations and our model, the probability of the i^{th} particle’s scattering is

$$P_i = \rho_i \sigma_{\text{scatt}} v_{\text{rel}} \Delta t. \quad (7)$$

ρ_i is the local density, v_{rel} the relative velocity between the i^{th} particle and its nearest neighbor, and Δt the time-step.

First, consider the local density. As mentioned, in Randall et al. the initial conditions are that the two merging components have King density profiles, $\rho(r) = \rho(0) [1 + (r/r_c)^2]^{-3/2}$, whereas our density profile is as in Figure 2. Two points defuse this concern. One, Randall et al. also simulate the collision of a King and a Hernquist density profile, leading them to claim their results are only weakly-dependent on the initial mass profiles. Two, the average density in our core is $\sim .6$ that in the King core. This suggests that the maximum allowed scattering cross section in our model would differ by an order unity factor from the bound quoted above at worst. As we will show, this bound would have to be orders of magnitude greater than what it is to permit bosonic repulsive DM in thermal equilibrium. Hence an order unity change in the bound would not alter our conclusion.

Now, consider the relative velocity, which in our model might be expected to differ from that in Randall et al.’s because in the core the DM is in a condensate governed by the Gross-Pitaevskii or non-linear Schrödinger equation. However, as we note in §5.3, there is a minimum DM particle mass for thermal equilibrium to have been reached by now. This minimum mass implies the maximum thermal de Broglie wavelength possible for the DM particle is $\sim .5 \text{ km}$. This is the scale on and below which quantum effects, such as the macroscopic shared wave-function of the particles, governed by the GP Equation, become significant. Clearly, it is far smaller than what would be resolved by a simulation. Hence, an N-body simulation of the DM we consider here

would not differ in this respect from Randall et al.’s—the GP Equation’s dynamics would simply not be important on a cosmological scale, except as encoded in the halo density profile, an issue already dealt with above.

Still on the subject of the relative velocity, it has been pointed out that two interpenetrating streams of pure RDM condensate will not scatter from one another and dissipate if their relative velocity is less than $v_{\text{crit}} = \sqrt{2U_0\rho/m^2}$ for the same reasons as in a conventional superfluid (Goodman 2000). Despite this, the Bullet Cluster constraint still applies. If K is chosen so that the minimum core radius of a dwarf galaxy is $\sim 1 \text{ kpc}$, then the critical velocity there will be comparable to the circular velocity at the edge of the core, $v_c \lesssim 100 \text{ km s}^{-1}$. From these values of v_c and r_c , one infers a typical dark-matter density $\rho_c \sim 20 m_H \text{ cm}^{-3}$ ($\approx 0.5 M_\odot \text{ pc}^{-3}$). The critical velocity in clusters will be lower because of the lower mass density, $\lesssim 1 m_H \text{ cm}^{-3}$.

Now, Randall et al. estimate v_{rel} for the Bullet Cluster as 4700 km s^{-1} , while Springel and Farrar (2007) estimate 2860 km s^{-1} . Either is much larger than v_{crit} . Hence there is no question that the RDM particles will scatter each other, rather than the two merging components frictionlessly interpenetrating each other as would be the case were $v_{\text{rel}} < v_{\text{crit}}$. Indeed, for $v_{\text{rel}} > v_{\text{crit}}$, as it is here, it is likely that the coherent state of the particles would be destroyed; the DM would no longer be in a condensate. Nonetheless, subsequent to the merger it might cool to reach gravitational equilibrium and in the process re-condense.

Finally, our discussion would be incomplete without acknowledging several other upper bounds on σ/m . Bradač et al. (2008) use the merging cluster MACS J0025.4–1222 in similar fashion to the Bullet Cluster and obtain the order-of-magnitude estimate $\sigma/m < 4 \text{ cm}^2 \text{ g}^{-1}$. It is worth noting that even were this looser limit used, it would still be too low to permit bosonic repulsive DM in thermal equilibrium. Other more stringent limits are available, however. Miralda-Escudé (2002) combines ellipticity measurements with the fact that DM collisions isotropize the DM’s stress-energy tensor and hence lead to more spherical galaxies. He finds $\sigma/m < .018 \text{ cm}^2 \text{ g}^{-1}$. As we discuss in §5.2, σ/m must be $\sim 1 \text{ cm}^2 \text{ g}^{-1}$ to allow local and global thermodynamic equilibrium, which our work will require. Hence, if Miralda-Escudé’s bound truly holds, it is an independent reason to doubt that DM can be in thermal equilibrium. Lin et al. (2011) present another bound also using the idea that only limited isotropization is observationally acceptable; it is $\sigma/m < .0025 \text{ cm}^2 \text{ g}^{-1}$. This bound too offers reason to doubt that DM can be in thermal equilibrium.

Nonetheless, given the uncertainties associated with limits on DM’s self-interaction cross section, in this paper we have chosen to adopt the view that repulsive, bosonic DM in thermal equilibrium may still be possible, and must be more fully considered before it can be decisively judged.

2.3 Pressure

Our main conclusions depend upon certain expected properties of the finite-temperature equation of state (hereafter EOS). Before presenting mathematical details, we address the general physical regime that we expect for this hypothetical RDM gas.

The limits of §2.2 imply that the interaction energy

4 Slepian and Goodman

between any single pair of particles is $\ll mv_c^2$, v_c being a characteristic virial or circular velocity. However, the *total* energy of interaction between a given particle and all of its neighbors is $\sim mv_c^2$ in the core where repulsion balances gravity. To match observed rotation curves, the halo should have an extended, approximately power-law envelope where the density is much lower than in the core. If the collisionality, though weak, suffices to establish local thermal and hydrostatic equilibrium (§5.2), the envelope must be supported mainly by microscopic thermal motions rather than the interparticle repulsion since the latter scales with the density. Hence the temperature in the envelope must be virial, $k_B T \sim mv_c^2$. We take the temperature of the gas to be the same in the halo as in the envelope. This is done partly for simplicity, but the limits above imply that the collisional mean-free path is comparable to the size of the galaxy, if not larger, so thermal conduction should be efficient. Finally, the repulsive interaction has a very short range, because we assume that it derives from a momentum-independent quartic potential of a complex scalar field. This range is much smaller than the thermal de Broglie wavelength

$$\Lambda_{\text{dB}} \equiv \frac{h}{\sqrt{2\pi m k_B T}}, \quad (8)$$

which in turn is much smaller than galactic scales unless the particle is extremely light.

With these assumptions, the RDM should behave as a nearly ideal boson gas, a type of system that has been studied extensively in connection with superfluidity and Bose-Einstein condensates. At least to first order in perturbation theory, the short-range two-body repulsion can be represented by a contact potential $U_0 \delta^{(3)}(\mathbf{r}_1 - \mathbf{r}_2)$ described by the single parameter U_0 , or equivalently, the “scattering length”

$$l = \frac{mU_0}{4\pi\hbar^2}. \quad (9)$$

This is not to be confused with the collisional mean-free path, which depends on density. In the first-Born approximation, $l = (\sigma_{\text{scatt}}/8\pi)^{1/2}$. The weakness of the individual pairwise interactions is expressed by $l \ll \Lambda_{\text{dB}}$.

Even with the idealization of a contact potential, the thermodynamics of a boson gas has not been solved exactly. Proukakis & Jackson (2008, hereafter PJ) review many of the approximations that have been used. The one we have adopted is what PJ call “Hartree-Fock” (HF). In this approximation, the gas is described by the occupation numbers of single-particle states—in our case, plane-wave momentum states, since Λ_{dB} is much smaller than scales on which the density or pressure varies. The grand-canonical partition function and pressure are derived semiclassically along lines similar to textbook derivations for a non-interacting boson gas. Some tricks are used to incorporate the interactions, as detailed in Appendix A.

At a given temperature T and particle mass m , the critical density above which the condensate appears in a non-interacting gas is²

$$\nu_{\text{crit}} = \zeta\left(\frac{3}{2}\right) \Lambda_{\text{dB}}^{-3} \approx 2.6 \Lambda_{\text{dB}}^{-3}, \quad (10)$$

² We use ν for number per unit volume and reserve n for mode occupation number.

i.e. approximately one particle per cubic de Broglie wavelength. In our HF approximation, the critical density for the condensate is also given by eq. (10).

The HF equation of state behaves as expected in highly degenerate and dilute limits, respectively $\nu \gg \nu_{\text{crit}}$ and $\nu \ll \nu_{\text{crit}}$. In the dilute limit, one recovers the pressure of an ideal gas because the repulsion becomes negligible. In the opposite limit, the HF approximation gives the polytropic equation of state $P = K\rho^2$, as does every approximation that is consistent with the Gross-Pitaevskii equation (41).

The HF approximation is least accurate in an intermediate regime where the condensate is present and the repulsive and thermal energies per excitation are comparable, $\nu U_0 \sim k_B T$ (see Pethick & Smith 2002). In such cases, the thermal excitations are not well described by single particles but rather by collective oscillations—quasiparticles. The dispersion relation for these excitations is eq. (42), which follows from linearisation of the Gross-Pitaevskii equation (41). It can be shown that our HF approximation effectively replaces eq. (42) with (neglecting the gravitational term)

$$\hbar\omega_k = \nu U_0 + \frac{(\hbar k)^2}{2m}. \quad (11)$$

If this were correct, there would be a minimum energy for the excitations (viz. νU_0) even at zero momentum, whereas the more correct relation (42) shows that the excitations with wavenumber $k \ll 2mc_s/\hbar \equiv k_s$ behave as phonons—quantized sound waves—with effective sound speed $c_s = \sqrt{\nu U_0/m}$. These phonons are not conserved: they are excited and damped by 3-mode nonlinear interactions that are not part of our HF approximation (which does however incorporate particle-conserving 4-mode interactions).

In order to assess the consequences of neglecting the quasiparticles for our equation of state, it is useful to introduce a dimensionless parameter that compares the repulsive and thermal energies at the critical density:

$$\theta = \frac{U_0 \nu_{\text{crit}}}{k_B T} = 2\zeta\left(\frac{3}{2}\right) \frac{l}{\Lambda_{\text{dB}}}. \quad (12)$$

The limits on collisionality from the Bullet Cluster imply that $\theta \ll 1$; in fact, using eqs. (2), (5), and (21) to eliminate U_0 , m , and T in favor of r_c , $v_{c,\infty}$ (the asymptotic halo velocity) and σ_{scatt}/m , one finds

$$\begin{aligned} \theta &= 2^{-12/5} \pi^{-1/10} \zeta\left(\frac{3}{2}\right) \left[\frac{\hbar v_{c,\infty}^5}{G^3 r_c^6} \left(\frac{\sigma_{\text{scatt}}}{m}\right)^4 \right]^{1/5} \\ &\approx 7 \times 10^{-21} \times \left(\frac{v_{c,\infty}}{100 \text{ km s}^{-1}}\right) \left(\frac{r_c}{1 \text{ kpc}}\right)^{-6/5} \left(\frac{\sigma_{\text{scatt}}/m}{1.25 \text{ cm}^2 \text{ g}^{-1}}\right)^{4/5} \end{aligned} \quad (13)$$

An independent reason to expect θ to be small is the assumption that RDM is the nonrelativistic limit of a charged scalar field with interaction term $\lambda|\phi|^4$ (see Kapusta & Gale 2006 for discussion of this formalism): if $U_0 = \lambda\hbar^3/4m^2c$, then

$$\theta = \lambda \frac{\zeta(3/2)}{16\pi^{3/2}} \left(\frac{v_{c,\infty}}{c}\right) \approx 10^{-5} \times \left(\frac{v_{c,\infty}}{100 \text{ km s}^{-1}}\right) \lambda, \quad (14)$$

and λ must be less than unity in order that perturbation theory make sense for the relativistic theory.

Let us compare the maximum energy of a phonon-like excitation, $\epsilon_s = \hbar c_s k_s = mc_s^2$, with the typical thermal excitation energy, $k_B T$. We find from the correct dispersion rela-

tion (42) that thermal excitations will be more like free particles (i.e. $\epsilon \approx (\hbar k)^2/2m$) than phonons unless $\nu \gtrsim \theta^{-1}\nu_{\text{crit}}$.

At high densities satisfying the latter condition, the phonon pressure has the Debye form

$$P_{\text{ph}} \approx \frac{\pi^2}{90} \frac{(k_{\text{B}}T)^4}{(\hbar c_s)^3}. \quad (15)$$

We can compare this with the pressure of the unexcited condensate, $P_0 = U_0\nu^2/2$. One finds that $P_{\text{ph}} \leq P_0$ when $\nu \gtrsim 2.0\theta^{-5/7}\nu_{\text{crit}}$.³ For $\theta \ll 1$, this minimum is lower than the density at which eq. (15) is valid. That means that for any density for which the thermal excitations are more like phonons than free particles (and the latter are already dealt with in our HF approximation), the pressure due to them will be less than the pressure of the unexcited condensate. In other words, the *thermal* contribution to the pressure is dominated by quasiparticles rather than “free” particles only when the density is so high that the total pressure is well-approximated by the zero-temperature relation $P = K\rho^2$ anyway.

In summary, since θ must be small to satisfy the Bullet Cluster constraint (see eq. (14)), we may neglect the quasiparticles and use the HF approximation of Appendix A to calculate the pressure as a function of density and temperature in RDM halos.

After these preliminaries, we now present our approximate equation of state in terms of a scaled pressure $\hat{P} = P/\nu_{\text{crit}}k_{\text{B}}T$, a scaled total number density $\hat{\nu} = \nu/\nu_{\text{crit}}$, and a scaled number density in the condensate $\hat{\nu}_0 = \nu_0/\nu_{\text{crit}}$. In terms of these parameters, the equation of state is

$$\hat{P} = \left(\hat{\nu}^2 - \frac{1}{2}\hat{\nu}_0^2 \right) \theta + \frac{\text{Li}_{5/2}(z)}{\zeta(3/2)}, \quad (16)$$

with

$$\hat{\nu} = \frac{\text{Li}_{3/2}(z)}{\zeta(3/2)} + H(\hat{\nu}_0) \quad (17)$$

and

$$z = \exp[-\theta\hat{\nu}_0], \quad \hat{\nu}_0 > 0. \quad (18)$$

H is the Heaviside function (0 for $\hat{\nu}_0 < 0$, 1 for $\hat{\nu}_0 > 0$). When $\hat{\nu}_0 = 0$, z is defined implicitly by eq. (17).

A log-log plot of the equation of state (eq. (16)) is shown in Figure 1 for $\theta = 1$, corresponding to strong scattering (although the steps leading to eq. (16) cannot be justified unless $\theta \ll 1$) and for $\theta = 10^{-4}$, corresponding to moderately weak scattering. The condensate is absent along the red section, and present along the blue. The part of the curve beneath the dashed line segment is unphysical; it can be shown that the integral of $\hat{P}d\hat{\nu}$ vanishes when taken around the loop defined by the dashed segment and the unphysical lobe below it. The endpoints of the dashed segment define two phases in contact, and the density jump at the phase transition scales $\propto \theta$ when $\theta \ll 1$. The actual phase transition is rather weak in the weakly interacting regime ($\theta \ll 1$) where our equation of state is valid.

We know from the discussion above that this equation of state is only approximate. What matters for the computation of halo rotation curves, however, is the following

³ The numerical constant is actually $[8\pi^{11}/(45\zeta(3/2))^2]^{1/7}$.

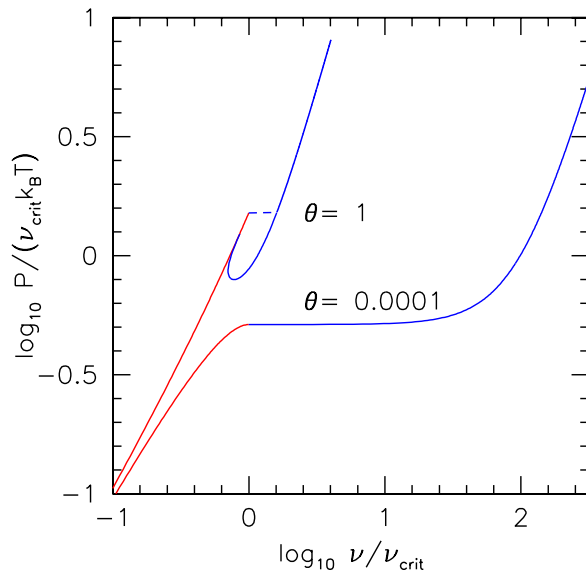


Figure 1. A log-log plot of scaled pressure $\hat{P} \equiv P/\nu_{\text{crit}}k_{\text{B}}T$ versus scaled number density $\hat{\nu} \equiv \nu/\nu_{\text{crit}}$ for interaction strengths $\theta = 1$ and $\theta = 10^{-4}$ (eq. (16)). The red curve is when no condensate is present, and the blue curve (only that to the right of and above the dashed line for $\theta = 1$) is when the condensate is present. For $\theta = 1$, the loop below the dashed line is unphysical: as the pressure increases beginning around $\log_{10} \hat{P} = .2$, the density experiences a large jump. For $\theta = 10^{-4}$, the pressure barely varies over a large range in density; this leads to the sudden drop in the density profile seen in Figure 2.

property that the foregoing assures us is shared by the exact EOS: when $\theta \ll 1$, the pressure supplied by the condensate is very small at the critical density compared to the pressure supplied by the non-degenerate component, and the latter is approximately that of a non-interacting gas. Therefore, as the pressure increases by a modest factor above its value at ν_{crit} —as it doubles, for example—the density must increase by a large factor $\sim \theta^{-1/2}$. This property of the EOS, together with the assumption of hydrostatic equilibrium, leads to a large jump in dark-matter density near the edge of the degenerate core.

3 DENSITY PROFILES FOR AN ISOTHERMAL SPHERICAL HALO

Using the equation of state, we solve the equations of hydrostatic equilibrium

$$\frac{dP}{dr} = -\frac{GM_r\rho}{r^2} \quad (19)$$

and

$$\frac{dM_r}{dr} = 4\pi\rho r^2 \quad (20)$$

The isothermal spherical halo we obtain thereby is the simplest model for a dark matter halo in virial equilibrium that has the correct flat rotation curve asymptotically. At large radii where the density is sufficiently small, the pressure $P \rightarrow \nu k_B T = \rho k_B T/m$, so that the solution tends to a classical isothermal sphere:

$$\begin{aligned} \rho(r) &\rightarrow \frac{k_B T}{2\pi G m} r^{-2}, & \text{and} \\ \frac{GM_r}{r} &\rightarrow \frac{2k_B T}{m} \equiv v_{c,\infty}^2 & \text{as } r \rightarrow \infty. \end{aligned} \quad (21)$$

This will provide an asymptotically flat rotation curve with amplitude $v_{c,\infty}$. Within the core ($r < r_c$), the condensate dominates, and the density profile is similar to that for an $n = 1$ Emden polytrope. This is unsurprising because for a pure condensate the equation of state is just that for an $n = 1$ polytrope. The inferred contribution of dark halos to the rotation curves of observed galaxies leads us to expect that the asymptotic velocity $v_{c,\infty}$ should be within a factor ~ 2 of the circular velocity v_c at the edge of the core (eq. (3)). This connects the temperature—or more precisely, the ratio T/m —to the sound speed at the center of the degenerate core, which depends in our model only upon the zero-temperature limit of the equation of state: $c_s^2(0) = 2K\rho(0)$. At intermediate radii however, as can be seen from Figure 2, the density profile and circular velocity are quite different from the classical isothermal sphere and depend strongly on the interaction parameter θ .

All models shown are scaled to the same central density, core radius and asymptotic rotation velocity or velocity dispersion; this demands that the scaled central number density $\hat{\nu}(0) = C\theta^{-1}$, C a constant. The reason for this is as follows. The physical central density $\rho(0) = m\nu_{\text{crit}}\hat{\nu}(0)$. Eliminating ν_{crit} in favor of θ via eq. (12), U_0 in favor of r_c^2 via eq. (2), and finally $k_B T/m$ via eq. (21) yields $\rho(0) = (\pi v_{c,\infty}^2/8Gr_c^2)C$. On the other hand, $\rho(0) = (\pi v_c^2/4Gr_c^2)$ from eq. (3). Thus the asymptotic circular velocity is related to the circular velocity at the edge of the core by $v_{c,\infty} = v_c\sqrt{2/C}$. Typical dwarf-galaxy rotation profiles suggest that $v_{c,\infty}$ should be modestly greater than v_c , so we set $C = 1$. We thus have a family of density profiles that depends only on θ , the interaction strength of the RDM, as demonstrated by Figure 2.

Perhaps surprisingly, it is the most strongly interacting model ($\theta = 1$) that most closely resembles the classical case. At $\theta \ll 1$, the density drops sharply outside the core, by a factor $\sim \theta$. It is then nearly constant out to $r \approx r_c/\sqrt{\theta}$. This occurs because, as discussed in §2.3, the pressure of the condensate is proportional to $\theta(\nu/\nu_{\text{crit}})^2$; the condensate would not contribute to the pressure at all if $\theta = 0$ (a noninteracting gas). In the limit $\theta = 0$, the pressure of the non-degenerate component, and therefore the total pressure, is independent of density once $\nu > \nu_{\text{crit}}$; increases in density merely increase the fraction of the particles in the condensate. If θ is small, the density must increase above ν_{crit} by a factor $\sim \theta^{-1/2}$ in order to double the pressure. Hence in hydrostatic equilibrium, a very large increase in density must occur over a small range in radius at the edge of the region where the condensate exists. The structure of the low- θ halos in Fig. 2 is reminiscent of a red giant, where the central

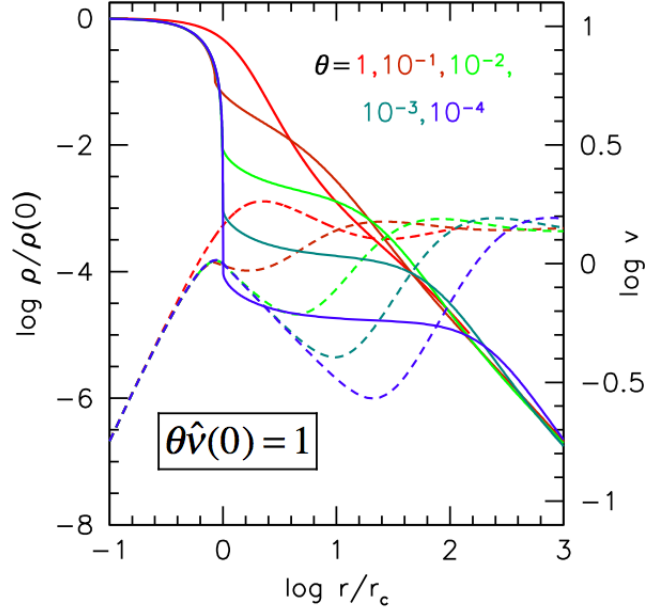


Figure 2. Self-gravitating isothermal spheres of RDM for various interaction strengths θ (eq. (12)). Solid curves and left axis: log-log mass density. Dashed curves and right-hand axis: log-log rotation curves. Notice the severe drops in the density profile for $\theta \ll 1$; these come from the small change in pressure over a large range in density we point out in Figure 1, and lead to the constraint that $\theta \geq 10^{-4}$ for realistic rotation curves.

parts are supported by degeneracy pressure and there is a distended envelope due to the large entropy increase across the hydrogen-burning shell.

This density drop is a key feature of our model because it leads to a dip in the rotation curve at the edge of the core. For $\theta = 10^{-4}$, the velocity dips by a factor ~ 2 , and for smaller values of θ the dip is even more pronounced. Such features appear to conflict with the inferred contribution of dark matter to galactic rotation curves. Therefore, if RDM halos really were isothermal, we would surely require $\theta \geq 10^{-4}$.

Requiring $\theta \geq 10^{-4}$ leads to a lower bound on the mass of the RDM particle.⁴ Replacing $(2k_B T/m)^{1/2}$ with the asymptotic circular velocity (21) yields $\Lambda_{\text{dB}} \approx \sqrt{4\pi\hbar/m\nu_{c,\infty}}$, which we insert into the definition (12) of θ . We relate l in that equation to U_0 via eq. (9) and U_0 to r_c via eq. (2). These manipulations yield

$$\theta \approx \zeta\left(\frac{3}{2}\right) \frac{Gm^4 r_c^2 v_{c,\infty}}{\pi^{5/2} \hbar^3}. \quad (22)$$

Requiring that $\theta \geq 10^{-4}$ means

$$m \geq 10. \times \left(\frac{v_{c,\infty}}{100 \text{ km s}^{-1}}\right)^{-1/4} \left(\frac{r_c}{1 \text{ kpc}}\right)^{-1/2} \text{ eV}/c^2. \quad (23)$$

⁴ Kouvaris & Tinyakov (2011) provide a lower limit on the mass and cross section of bosonic self-interacting DM using neutron star observations, but theirs is not in conflict with the Bullet Cluster upper bound. Hence our more stringent bound from the rotation curves is needed to see that the DM in thermal equilibrium we consider here is untenable.

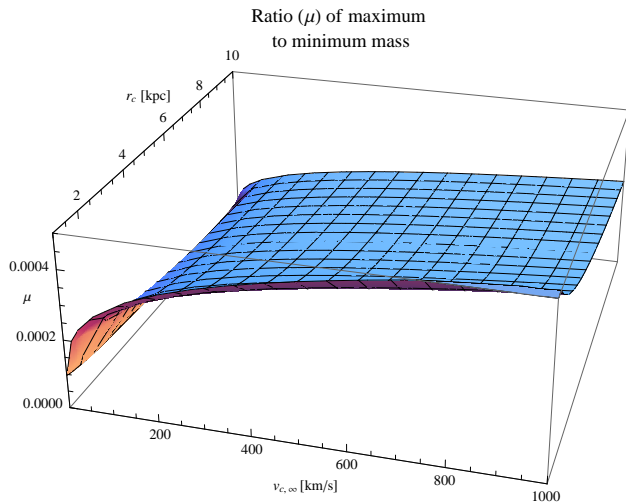


Figure 3. Plot of ratio μ of maximum to minimum mass from two constraints eqs. (6) and (23); horizontal axes are v_c in km/s (front) and r_c in kpc (left-hand side). For a viable model, clearly the maximum mass must be greater than the minimum mass, so we would require $\mu \geq 1$. This is not achievable over the realistic parameter space for v_c and r_c .

Table 1. Symbols used in this work

ν	number density
$\hat{\nu}$	scaled number density
ν_0	condensate number density
ν_{crit}	density where cond. appears
θ	interaction parameter
r_c	halo core radius
v_c	halo circular velocity
U_0	Fourier transform of pot'ial at $\vec{p} = 0$
m	RDM particle mass
σ_{scatt}	RDM particle scattering cross sxn.
l	scattering length
Λ_{dB}	RDM de Broglie wavelength

4 RULING OUT RDM IN THERMAL EQUILIBRIUM

Consider jointly eqs. (6) and (23). As r_c increases, the lower bound on m will fall, but evidently so will the upper bound, so we cannot hope to leave v_c fixed and tune r_c such that both constraints are satisfied. Could we leave r_c fixed and raise v_c enough so that eq. (23) aligns with eq. (6)? Certainly not; since eq. (23) depends so weakly on v_c , to achieve this would demand $v_c \simeq 10^{16} \text{ km s}^{-1}$, considerably in excess of the speed of light! Figure 3 shows the ratio $\mu \equiv \max(m)/\min(m)$; for a viable dark matter particle it has to be greater than or equal to unity, which it clearly is not over the realistic parameter space for v_c and r_c .

5 DISCUSSION AND CONCLUSIONS

5.1 Context for our work

As we note in the Introduction, self-interacting, bosonic dark matter models have been considered before. For a detailed review of the history of work on astrophysical-scale bosonic objects, e.g. boson stars (first proposed by Kaup (1968) and Ruffini & Bonazzola (1969)), as well as galactic halos (first suggested by Baldeschi et al. (1983)), we refer the reader to Chavanis 2011. Here, we review what is necessary to contextualize our own work.

As Chavanis notes, Baldeschi et al. considered the possibility that DM halos might be composed of a non-degenerate component and a condensate. However, in this model and subsequent studies (e.g. Sin 1994), the possibility of self-interaction was ignored. Many scalar field models (Schunck 1998, Matos & Guzman 1999, see Chavanis 2011 for further discussion) were proposed that also assumed no self-interaction. These models all required small masses ($m \sim 10^{-24} \text{ eV}/c^2$) to achieve a sufficiently large core radius in agreement with observation. To avoid this “unnaturally small mass,” self-interaction was proposed: see Colpi et al. 1986, Lee & Koh 1996, and Arbey et al. 2003, as well as the references mentioned in the Introduction.

Goodman (2000) pointed out that this would lead to a minimum halo core size $r_c = 3\sqrt{U_0/4\pi Gm^2}$, and Lee & Lim (2010) show that there is also a minimum mass, $M_{\text{min}} \simeq \hbar^2/G\lambda_c m^2$, with λ_c the DM particle’s Compton wavelength. Rindler-Daller & Shapiro (2010) observe that vortices should form for a strongly self-interacting condensate, and that this may affect the density profile (2011). Bohmer & Harko (2007) pick up where Goodman left off and calculate rotation curves for a repulsive, completely Bose-Einstein condensed halo, noting that the gravitational lensing prediction differs from CDM. However, as Chavanis comments, they ignore the quantum pressure, i.e. the additional pressure due to Heisenberg uncertainty. Chavanis therefore connects the non-interacting (but including quantum pressure) limit of Ruffini & Bonazzola (1969) with the interacting (but no quantum pressure) limit studied by Bohmer & Harko (2007), taking into account both the quantum pressure and a repulsive (or attractive) self-interaction.⁵ Chavanis obtains both analytical (paper I) and numerical (paper II) mass profiles and rotation curves. However, his work does not treat the case where the DM has a non-zero temperature and there are both condensed and non-condensed components present. This is the gap our paper fills.

We would note that it is an important gap because as it turns out, the presence of a non-condensed component is what leads to the abrupt density drop in the halo profile (see Figure 2). This abrupt drop in turn leads to unrealistic rotation curves and so places a lower bound on the collisionality of the RDM (lower collisionality implies a steeper density drop). It is the combination of this constraint with

⁵ We neglect the quantum pressure because for it to be significant would require a mass so small as to have a Compton wavelength comparable to the core radius ($m \sim \hbar/r_c v_c \sim 10^{-22} \text{ eV}$), as with Hu et al.’s (2000) “fuzzy dark matter.” This would be the type of “unnaturally small mass” that self-interaction was originally introduced to avoid.

that the Bullet Cluster places on the scattering cross section that allows us to rule out repulsive, bosonic dark matter in thermal equilibrium. Hence we can conclude that the effects of non-zero temperature are in fact critical to understanding the behavior of a bosonic, repulsive DM model in thermal equilibrium.

5.2 Thermal Equilibrium

Before closing, there are four issues we should briefly address. First, as we noted in the Introduction, the conclusion we have presented can be avoided if the DM has not reached thermal equilibrium either locally or globally. For our equation of state to be valid, we require local thermodynamic equilibrium, reached via collisions on a timescale $t_{\text{coll}} \sim \lambda_{\text{mfp}}/v_c$. For our isothermal halo models to be valid, we also require global thermodynamic equilibrium, reached via conduction on a timescale $t_{\text{cond}} \sim r^2/v_c\lambda_{\text{mfp}}$, where r is the radius of the DM halo and we estimate $r \sim r_c$. So unless t_{coll} and t_{cond} are both much less than the Hubble time t_{H_0} , our halo models are invalid, in which case so is the constraint eq. (23), as it comes from demanding that the drop in the halo density profile not be too steep.

If $\sigma_{\text{scatt}}/m \approx 1 \text{ cm}^2 \text{ g}^{-1}$ (near the upper end of the range allowed by the Bullet Cluster), then $r \sim \lambda_{\text{mfp}}$ in the solar neighborhood, and $t_{\text{coll}} \sim t_{\text{cond}} \ll t_{H_0}$ so we have both local and global thermodynamic equilibrium. But if σ_{scatt}/m were significantly smaller than this value, the dark matter would not undergo sufficient scattering to reach local thermodynamic equilibrium (i.e. $t_{\text{coll}} > t_{H_0}$). This would invalidate our equation of state, and place us effectively in the limit of a non-interacting, axion-like particle. There would be one salient difference from the non-interacting axion even in this regime, however: the collective repulsion could still provide a core, since as we have pointed out earlier, the collisionality and minimum core size are independent. In short, in this limit, the upper bound eq. (6) on the mass still applies, but the lower bound eq. (23) does not.

5.3 Supporting the degenerate core

Second, we reiterate here that there is no conflict between a small interaction parameter θ and a large core, $r_c \gg \Lambda_{\text{dB}}$, because the de Broglie wavelength, core radius, and interaction parameter depend upon the particle mass m and scattering length l in different combinations. From eq. (12) we have that $\theta \sim l/\Lambda_{\text{dB}}$. (To avoid distraction from the important scalings dimensionless factors of order unity are suppressed here.) The temperature T of the hypothetical RDM is not observable, but $k_{\text{B}}T/m \sim v_c^2$ is observable, v_c being a characteristic circular velocity. Thus $\Lambda_{\text{dB}} \sim h/mv_c$ and $\theta \sim mlv_c/h$. On the other hand, eliminating U_0 from the core radius (2) in favor of the scattering length (9) gives $r_c \sim (\hbar^2 l/Gm^3)^{1/2}$. So at a fixed value of v_c , we have $\Lambda_{\text{dB}} \propto m^{-1}$, $\theta \propto ml$, and $r_c \propto l^{1/2}m^{-3/2}$. Eliminating the scattering length between these relations and including the numerical factors produces eq. (22), which clearly shows that one can have an arbitrarily small θ at any given r_c for sufficiently small particle mass.

If the mass were as small as $h/r_c v_c \sim 10^{-22} \text{ eV}/c^2$, then the de Broglie length would be comparable to the core ra-

dius; for masses smaller than this, the core would be supported by “quantum pressure” even without repulsive interactions. However, as eq. (6) and the discussion in §5.2 indicate, the scattering cross section is insufficient to establish thermal equilibrium at galactic densities over a Hubble time if the particle mass is much smaller than $10^{-3} \text{ eV}/c^2$. Thus there is a wide range of masses—some 19 orders of magnitude—over which the cores of galaxies could be supported by repulsion rather than a large de Broglie wavelength and yet two-body collisions would be totally ineffective at thermalizing their distribution. This regime, however, is not the main focus of the present paper.

5.4 Vortices

Third, we consider whether the vortex formation Rindler-Daller & Shapiro (hereafter RDS) (2010) claim will occur in strongly self-interacting Bose-Einstein condensed DM would possibly change the rotation curve (RDS 2011) in a way to avoid the constraint we use here.

Some care is required. RDS (2011) derive two constraints that both must be independently satisfied for vortices to form: a minimum mass, and a minimum interaction strength. At first blush, we might take the minimum mass of eq. (23) and ask whether it exceeds their required minimum.

However, this approach would be subtly flawed: the minimum mass of eq. (23) is based on the observationally disallowed density profile it would produce. But this density profile assumes no vortices are present. Hence, the minimum mass it implies is not the correct lower bound if vortices form. Indeed, if vortices form, they would form only in the condensate core of the halo, and lower the density there while minimally affecting the non-degenerate envelope’s density.⁶ So at a given θ , the “cliff” in the density would be smoothed out—thus allowing a lower minimum value of θ to be consistent with observation than if vortices are not considered. Since $m \propto \theta^{1/4}$ from eq. (22), this would lower the minimum allowed mass of eq. (23).

Indeed, it is worthwhile to ask just how much vortices could lower this minimum allowed mass of eq. (23). In particular, could they lower it enough so that it became less than the maximum mass of eq. (6), thereby saving repulsive dark matter in thermal equilibrium from being ruled out by the mismatch of these constraints? To get the constraints to match would require lowering the lower bound eq. (23) by a factor of 10^{-5} , and hence θ by a factor of 10^{-20} . So the vortices would have to deplete the core density enough that a density profile corresponding to $\theta \simeq 10^{-24}$ was observationally allowed.

Even with the mass lower by a factor of 10^{-5} , $\Lambda_{\text{dB}} \ll r_c$, so the contribution of quantum pressure to supporting the core would still be negligible. Thus the core would still need to be supported by repulsion alone. But $\theta \geq 10^{-9}$ is required to fulfill this condition. So if the vortices could deplete the

⁶ RDS’s work is motivated by the fact that vortices form in BEC’s produced in the laboratory (see e.g. Madison et al. 2000); there is no reason to expect them to form in the non-degenerate component of the halo. The change in the density of the core would affect the gravitational potential experienced by the outer, non-degenerate envelope, but this effect would be at 2nd order.

core's density sufficiently to make our lower bound on m consistent with our upper bound, we would lose the degenerate core, the feature that motivated considering repulsive bosonic DM in the first place! In short, then, the presence of vortices will not affect our conclusion that repulsive bosonic DM in thermal equilibrium is observationally ruled out.

For the sake of completeness, we now deal with the question of whether vortices will indeed form. The minimum mass for which our model can be valid is $m \sim 10^{-3} \text{ eV}/c^2$ (see §5.3). This is larger than the largest minimum mass RDS 2011 requires for vortex formation, $m \simeq 10^{-21} \text{ eV}/c^2$.⁷ Using eq. (2) to relate U_0 to m and r_c , the minimum value of U_0 (which occurs at the minimum mass computed above) is $U_0 \simeq 10^{-22} \text{ eV cm}^3$. This is stronger than the largest minimum required repulsion of $2 \times 10^{-58} \text{ eV cm}^3$. Thus, vortices will form as long as the ancillary assumptions (e.g., non-zero spin parameter λ) made by RDS 2011 are satisfied.

However, it should be borne in mind that, as we have shown above, were vortices to form, if they depleted the core density enough to evade the conflicting bounds we place on the DM particle's mass, the observationally-required core would disappear. Thus, to reiterate, they do not affect our conclusion that repulsive bosonic DM in thermal equilibrium is observationally ruled out. Nonetheless, one might worry that if a vortex forms precisely at the center of the halo, then the scaling we have used throughout, $\hat{\nu}(0)\theta = C \equiv 1$ (see §3) would be invalid, as the density at the center of the vortex (and hence halo) would be zero. In response to this, it must be observed that the vortex will be quite small. Its size is given by the healing length, ξ (see RDS 2011, Fetter & Foot 2012 for details):

$$\xi = \frac{\hbar}{\sqrt{2U_0\rho}} \approx \frac{\hbar}{mv_c} \simeq .6 \text{ m}, \quad (24)$$

where we have used the definition of v_{crit} and then that $v_{\text{crit}} \simeq v_c$ to obtain the second and third equalities. Hence any vortex would be minuscule. In any case, were a vortex present at the center of the halo, one might simply replace our $\hat{\nu}(0)$ with $\langle \hat{\nu}(r < r_s) \rangle$, with r_s some smoothing length defining a sphere over which the average density (denoted by the angle brackets) is taken.

5.5 Drag on a rotating galactic bar

Finally, we consider the drag on a rotating galactic bar in our model. Since we have argued that bosonic repulsive dark matter in thermal equilibrium should be ruled out, this discussion is of secondary importance. We refer the reader to Appendix B for our treatment.

6 ACKNOWLEDGEMENTS

JG gratefully acknowledges the Chandrasekhar Centenary Conference for the opportunity to present an earlier version of this work; ZS expresses thanks to Dr. Gregory Novak for useful conversations during the course of this research.

⁷ See their (2011), Table 2; we use dwarf-galaxy values as they provide roughly the same radius and mass as the degenerate core where we are concerned to determine if vortices form.

ZS also thanks Tanja Rindler-Daller for helpful correspondence on vortices, David Spergel for discussion on the current state of observational DM research, and Neta Bahcall for intuition on the broad techniques used to determine DM masses. This material is based upon work supported by the National Science Foundation Graduate Research Fellowship under Grant No. DGE- 1144152. Finally, we are very grateful to the anonymous referee for many careful comments that significantly improved the substance of this work.

7 REFERENCES

- Ahn K and Shapiro P, 2005, MNRAS 363, 1092-1124, arXiv:astro-ph/0412169
- Amaro-Seoane P, Barranco J, Bernal A, Rezzolla L, 2010, JCAP 1011: 002, arXiv:1009.0019v2
- Annett JF, 2004, Superconductivity, Superfluids, and Condensates, Oxford: University Press
- Arbey A, Lesgourgues J, and Salati P, 2003, Phys. Rev. D 68, 023511, arXiv:astro-ph/0301533
- Baldeschi MR, Gelmini GB, and Ruffini R, 1983, Phys. Lett. B 122, 221
- Bekenstein JD, 2006, Contemporary Physics 47, 387, arXiv:astro-ph/0701848
- Bernal A, Matos T, and Nunez D, 2008, Revista Mexicana de astronomia y astrofisica, 44, 1, arXiv:astro-ph/0303455
- Bernal A, Guzman FS, 2006, Phys. Rev. D 74: 103002, arXiv:astro-ph/0610682
- Bertone G, Hooper D, and Silk J, 2005, Phys. Rept. 405: 279-390, arXiv:hep-ph/0404175v2
- Binney J and Tremaine S, 2008, Galactic Dynamics: Second Edition Princeton: Univ. Pr.
- Bohmer CG and Harko T, 2007, JCAP 0706:025, arXiv:0705.4158v4
- Bradač M et al., 2008, ApJ 687 959, <http://iopscience.iop.org/0004-637X/687/2/959/>
- Briscese F, 2011, arXiv:1001.0028v3
- Chavanis PH, 2011, Phys. Rev. D 84, 043531, arXiv:1103.2050v2
- Chavanis PH and Delfini L, 2011, Phys. Rev. D 84, 043532, arXiv:1103.2054
- Cole DR, Dehnen W, and Wilkinson MI, 2011, MNRAS 16, 2, 1118-1134, arXiv:1105.4050
- Colin P, Klypin A, Valenzuela O, and Gottlober S, 2004, ApJ 612, 50, arXiv:astro-ph/0308348
- Colpi M, Shapiro SL, and Wasserman I, 1986, Phys. Rev. Lett. 57, 2485
- Debattista VP and Sellwood JA, 1998, ApJ 493: L5-L8, arXiv:astro-ph/9710039
- Debattista VP and Sellwood JA, 2000, ApJ 543, 704-721, arXiv:astro-ph/0006275
- de Blok WJG, McGaugh S, Bosma A, and Rubin VC, 2001, ApJ 552, L23-26, arXiv:astro-ph/0103102
- Elson EC, de Blok WJG, and Kraan-Korteweg RC, 2010, MNRAS 404, 4, 2061-2076, arXiv:1002.0403v1
- Fetter AL and Foot CJ, 2012, arXiv:1203.3183v1
- Diemand J, Moore B, and Stadel J, 2005, Nature. 433, 389, arXiv:astro-ph/0501589

Geressen J, Kuijken K, and Merrifield MR, 1999, MNRAS 306, 926

Goldreich P and Nicholson PD, 1989, ApJ, 342, 1079

Guaenault AM, 2003, Basic Superfluids, New York: Taylor and Francis

Harko T, 2011, arXiv:1105.5189v1 (II)

Harko T, 2011, arXiv:1105.2996v1 (II)

Hennawi J and Ostriker J, 2002, ApJ, 572 41, arXiv:astro-ph/0108203

Hirota A et al., 2009, PASJ, 61, 441

Hu W, Barkana R, and Gruzinov A, 2000, Phys. Rev. Lett. 85, 1158, arXiv:astro-ph/0003365

Jardel JR and Sellwood JA, 2009, ApJ 691, 1300, arXiv:0808.3449

Kapusta JI and Gale C, 2006, Finite-Temperature Field Theory, Cambridge: University Press

Kaup DJ, 1968, Phys. Rev. 172, 1331

Koda J, Shapiro P, 2011, arXiv:1101.3097v2

Komatsu E et al., 2011, ApJS 192: 18, arXiv:1001.4538

Kouvaris C and Tinyakov P, 2011, PRL 107, 091301, arXiv:1104.0382

Lee J and Koh I, 1996, Phys. Rev. D 53, 2236, arXiv:hep-ph/9507385

Lee J-W, 2009, Journal of the Korean Physical Society, 54, 6, 2622, arXiv:0801.1442v4

Lee J-W and Lim S, 2010, JCAP 1001: 007, arXiv:0812.1342v3

Lin T, Yu H-B, and Zurek K, 2011, arXiv:1111.0293v1

Loeb A and Weiner N, 2011, Phys. Rev. Lett. 106: 171302, arXiv:1011.6374v1

Mandl F, 1988, Statistical Physics, Chichester: John Wiley & Sons

Merrifield MR and Kuijken K, 1995, MNRAS, 274, 933

Mikheeva E, Doroshkevich A, and Lukash V, 2007, Nuovo Cim. 122B, 1393, arXiv:0712.1688

Miralda-Escudé J, 2002, ApJ 564: 60-64, arXiv:astro-ph/0002050

Mitra S, 2005, Phys. Rev. D 71, 121302, arXiv:astro-ph/0409121v5

Mo HJ and Mao S, 2000, MNRAS 318, 163, arXiv:astro-ph/0002451v2

Peebles PJE, 1993, Principles of Physical Cosmology, Princeton: University Press

Pethick C and Smith H, 2002, Bose-Einstein Condensation in Dilute Gases, Cambridge: University Press

Pitaevskii L and Lifshitz EM, 1980, Statistical Physics. Part 2. Oxford: Pergamon

Proukakis N and Jackson B, 2008, J. Phys. B: At. Mol. Opt. Phys. 41 203002

Randall SW, Markevitch M, Clowe D, Gonzalez AH, and Bradac M, 2008, ApJ 679, 1173, <http://iopscience.iop.org/0004-637X/679/2/1173/fulltext/71772.text.html>

Rindler-Daller T and Shapiro P, 2010, New Horizons in Astronomy (Bash Symposium 2009), Proceedings of the Astronomical Society of the Pacific, eds. L Stanford, L Hao, Y Mao, J Green, arXiv:0912.2897v2

Rindler-Daller T and Shapiro P, 2011, arXiv:1106.1256v1

Riotto A and Tkachev I, 2000, Physics Letters B, 484, 177

Ruffini R and Bonazzola S, 1969, Phys. Rev. 187, 1767

Sahni V, 2004, Proceedings of the Second Aegean Summer School on the Early Universe, Syros, Greece, arXiv:astro-ph/0403324v3

Schunck FE, 1998, arXiv:astro-ph/9802258

Sin SJ, 1994, Phys. Rev. D 50, 3650

Spergel D and Steinhardt PJ, 2000, Observational evidence for self-interacting cold dark matter, arXiv:astro-ph/9909386v2

Springel V and Farrar G, 2007, MNRAS 308, 911-925.

Su K-Y, Chen P, 2011, JCAP08, 016, arXiv:1008.3717v2

Tolman RC, 1938, The Principles of Statistical Mechanics, Oxford: University Press

Tremaine S and Ostriker J, 1999, MNRAS 306, 662, arXiv:astro-ph/9812145

Urena-Lopez L, 2009, JCAP0901: 014, arXiv:0806.3093v2

Madison KW, Chevy F, Wohlleben W, and Dalibard J, 2000, Mod. Opt., 47, 2715

Matos T and Guzman FS, 1999, F. Astron. Nachr. 320, 97

Matos T and Urena-Lopez L, 2002, Phys. Lett. B 538, 246-250, arXiv:astro-ph/0010226

Wandelt BD, Davé R, Farrar GR, McGuire PC, Spergel DN, and Steinhardt PJ, 2000, Proceedings of Dark Matter, arXiv:astro-ph/0006344v2

8 APPENDIX A: EQUATION OF STATE

8.1 Partition function to pressure

Insofar as possible, we follow elementary treatments of a noninteracting ideal boson gas, describing microstates by the number of quanta $(n_0, n_1, \dots, n_k, \dots) \equiv \vec{n}$ in each single-particle momentum state $|k\rangle$. The total number and volume of the gas are $N = \sum n_k$ and V , respectively. The pairwise potential is so short range as to be represented by a constant, U_0 , in momentum space. The energy of microstate \vec{n} , including exchange terms, is then

$$E(\vec{n}) = \sum_k \frac{k^2}{2m} n_k + \frac{U_0}{2V} \left[N^2 + \sum_k \sum_{j \neq k} n_j n_k \right] \quad (25)$$

$$= \sum_k \frac{k^2}{2m} n_k + \chi \left[2 \sum_k n_k - N^{-1} \sum_k n_k^2 \right], \quad (26)$$

where $\chi \equiv NU_0/2V$ is proportional to the mean potential energy per particle. The grand-canonical partition function (GCPF) cannot be found by summing over the n_k independently, even at fixed χ , because of the terms $\propto -n_k^2/N$. In the thermodynamic limit, however, only the ground state can have a macroscopic occupation number (i.e., $\lim_{N \rightarrow \infty} n_0/N > 0$ at fixed N/V and β), for the usual reasons. Therefore, $N^{-1} \sum_k n_k^2$ can be replaced by $N^{-1} n_0^2$.

The canonical (not grand-canonical) partition function is

$$Z(\beta, V, N) = \sum_{n_0=0}^N Z_0(\beta, V, n_0) Z_{\text{nd}}(\beta, V, N - n_0), \quad (27)$$

in which Z_0 and Z_{nd} are the canonical partition functions (CPFs) of the ground single-particle state and of the remaining states, respectively (“nd” means “non-degenerate”). The

summand eq. (27) is sharply peaked either at $\bar{n}_0 = 0$, or at $n_0 = \bar{n}_0$ such that

$$\left. \frac{\partial \ln Z_0}{\partial n_0} \right|_{n_0=\bar{n}_0} = \left. \frac{\partial \ln Z_{\text{nd}}}{\partial N_{\text{nd}}} \right|_{N_{\text{nd}}=N-\bar{n}_0}, \quad (28)$$

if this has a solution for $\bar{n}_0 > 0$. Hence in the thermodynamic limit,

$$\ln Z(\beta, V, N) = \ln Z_0(\beta, V, \bar{n}_0) + \ln Z_{\text{nd}}(\beta, V, N - \bar{n}_0). \quad (29)$$

It remains to find Z_0 and Z_{nd} . Neglecting $p_0^2/2m = O(V^{-2/3}\hbar^2/m)$,

$$Z_0(\beta, V, n_0) = \exp[-\beta\chi(2n_0 - N^{-1}n_0^2)]. \quad (30)$$

Note that Z_0 depends implicitly on N through χ as well as N^{-1} .

To obtain Z_{nd} , we begin by finding the grand-canonical partition function (GCPF) for the non-degenerate states, which we denote \mathcal{Z}_{nd} ; it will lead to the canonical partition function Z_{nd} via eq. (33). Because the n_k^2 terms have been dropped for $k > 0$, it can be computed as for an ideal gas, with modal energies $\epsilon_k = p_k^2/2m + 2\chi$:

$$\begin{aligned} \ln Z_{\text{nd}}(\beta, V, \mu_{\text{nd}}) &= \sum_{k=1}^{\infty} \ln \left(\sum_{n_k=0}^{\infty} e^{-n_k\beta(\epsilon_k - \mu_{\text{nd}})} \right) \\ &\approx V\nu_{\text{crit}}(\beta)\zeta\left(\frac{3}{2}\right)^{-1}\text{Li}_{5/2}\left[e^{\beta(\mu_{\text{nd}} - 2\chi)}\right] \end{aligned} \quad (31)$$

The polylogarithm $\text{Li}_{5/2}$, which is equivalent to a Bose-Einstein integral, results from approximating the sum over k by an integral over p_k . The critical density $\nu_{\text{crit}}(\beta)$ is defined in eq. (10).

The quantity μ_{nd} is not the chemical potential of the full system, which would be conjugate to N , but instead describes the division of particles between the ground state and the rest:

$$\bar{N}_{\text{nd}} = \left(\frac{\partial \ln \mathcal{Z}_{\text{nd}}}{\partial \mu_{\text{nd}}} \right)_{\beta, V, N} = N - \bar{n}_0, \quad (32a)$$

$$\mu_{\text{nd}} = -\beta^{-1} \left(\frac{\partial \ln \mathcal{Z}_{\text{nd}}}{\partial \bar{N}_{\text{nd}}} \right)_{\beta, V, N}, \quad (32b)$$

both of which are implied by the thermodynamic relation

$$\ln Z_{\text{nd}}(\beta, V, \bar{N}_{\text{nd}}) = \ln \mathcal{Z}_{\text{nd}}(\beta, V, \mu_{\text{nd}}) - \beta\mu_{\text{nd}}\bar{N}_{\text{nd}}. \quad (33)$$

Recall that \mathcal{Z}_{nd} is the GCPF, not the CPF, but we require the CPF Z_{nd} . Here, the GCPF is only a device for obtaining the CPF.

Combining eqs. (28), (30), and (32b) yields

$$\mu_{\text{nd}} = 2 \left(1 - \frac{\bar{n}_0}{N} \right) \chi, \quad (34)$$

but only when \bar{n}_0 is macroscopic, since otherwise eq. (28) does not hold.

Combining eqs. (29), (30), (31), and (33):

$$\begin{aligned} V^{-1} \ln Z(\beta, V, N) &= -\beta\chi \left(2\nu_0 - \frac{\nu_0^2}{\nu} \right) - \beta\mu_{\text{nd}}(\nu - \nu_0) \\ &\quad + \nu_{\text{crit}}(\beta)\zeta\left(\frac{3}{2}\right)^{-1}\text{Li}_{5/2}\left[e^{\beta(\mu_{\text{nd}} - 2\chi)}\right], \end{aligned} \quad (35)$$

where the intensive variables $\nu \equiv N/V$ and $\nu_0 \equiv \bar{n}_0/V$ have been introduced. In this global CPF, μ_{nd} and ν_0 are

functions of (β, V, N) given by eqs. (32a) and (34) if \bar{n}_0 is macroscopic; else $\nu_0 \rightarrow 0$ and $\bar{N}_{\text{nd}} \rightarrow N$ in eq. (32a). More explicitly,

$$\begin{aligned} \nu &= \nu_0 + \nu_{\text{crit}}(\beta)\zeta\left(\frac{3}{2}\right)^{-1}\text{Li}_{3/2}\left[e^{-\beta U_0\nu_0}\right] & \nu > \nu_{\text{crit}}, \\ \nu &= \nu_{\text{crit}}(\beta)\zeta\left(\frac{3}{2}\right)^{-1}\text{Li}_{3/2}\left[e^{\beta[\mu_{\text{nd}} - U_0\nu]}\right] & \nu \leq \nu_{\text{crit}}. \end{aligned} \quad (36)$$

The pressure is now computable as

$$\begin{aligned} P &= \beta^{-1} \left(\frac{\partial \ln Z}{\partial V} \right)_{\beta, N} \\ &= \beta^{-1} \left[\left(\frac{\partial \ln Z_0}{\partial V} \right)_{\beta, \bar{n}_0} + \left(\frac{\partial \ln Z_{\text{nd}}}{\partial V} \right)_{\beta, N - \bar{n}_0} \right]. \end{aligned} \quad (37)$$

In the second line, \bar{n}_0 can be treated as constant because the terms involving $\partial\bar{n}_0/\partial V$ cancel from eq. (37) due to eq. (28). Similarly, terms involving $\partial\mu_{\text{nd}}/\partial V$ cancel from the derivative of Z_{nd} in the form of eq. (33) due to eq. (32a). But terms involving $\partial\chi/\partial V$ do matter. After some manipulation,

$$P = U_0 \left(\nu^2 - \frac{1}{2}\nu_0^2 \right) + \beta^{-1}\nu_{\text{crit}}(\beta)\zeta\left(\frac{3}{2}\right)^{-1}\text{Li}_{5/2}\left[e^{\beta[\mu_{\text{nd}} - U_0\nu]}\right]. \quad (38)$$

8.2 Limiting behavior

In this section, we show that the approximate equation of state defined by eqs. (16)-(18) has the expected behavior at both extremes of the degeneracy parameter $\nu/\nu_{\text{crit}}(T)$. The Hartree-Fock approximation is that the boson gas can be described in terms of occupation numbers of single-particle states, and the discussion below reflects this viewpoint—which, however, is not accurate at intermediate densities where quasiparticles dominate, as discussed in §2.3.

When $T = 0$, all of the DM particles will be in the lowest-energy state, corresponding to a pure Bose-Einstein condensate. This is evident from the fact that $\nu_{\text{crit}} \propto T^{3/2}$, so that $\nu_{\text{crit}} \rightarrow 0$ as $T \rightarrow 0$. The equation of state should reduce to the one given in §2.1, $P = K\rho^2 = U_0\nu_0^2/2$, which follows from the fact that there are $n^2/2$ pairs per unit volume and that the energy per pair is $U_0\delta(\mathbf{r}_1 - \mathbf{r}_2)$. The constant U_0 in P corresponds to the “bare” interaction only to first order; at higher orders in perturbation theory it must be renormalized.

In the argument of the polylogarithm in eq. (38), $\mu_{\text{nd}} - U_0\nu$, with $\nu = \nu_0$, simplifies to $-U_0\nu\bar{n}_0/N$, clearly independent of T . Thus that quantity remains negative as $T \rightarrow 0$. $\beta \rightarrow \infty$ as $T \rightarrow 0$, so the argument of the polylogarithm in eq. (38) becomes zero. The term multiplying it, $\beta^{-1}\zeta\left(\frac{3}{2}\right)$, also goes to zero. So the pressure becomes $P = U_0 \left(\nu^2 - \frac{1}{2}\nu_0^2 \right)$. Since $\nu = \nu_0$ because all of the DM is in the condensate, this reduces to $P = U_0\nu_0^2/2$ as required.

In the limit that $U_0 \rightarrow 0$, the gas is non-interacting and should approach an ideal gas of indistinguishable bosons. For a given ν , if T is such that $\nu \leq \nu_{\text{crit}}$, there will be no condensate, and the chemical potential μ_{nd} , which governs particles’ transition from the ground state to excited states, is determined by inverting eq. (36) ($\nu \leq \nu_{\text{crit}}$). Taking $U_0 = 0$ and rewriting the second term in eq. (38) using eq. (36) ($\nu \leq \nu_{\text{crit}}$), we have

$$P = \beta^{-1}\nu \frac{\text{Li}_{5/2}\left[e^{\beta\mu_{\text{nd}}}\right]}{\text{Li}_{3/2}\left[e^{\beta\mu_{\text{nd}}}\right]}. \quad (39)$$

This agrees with standard results (e.g. Tolman 1938). For an interacting gas in the dilute limit where the dimensionless combination $\beta U_0 \nu \rightarrow 0^+$, the same result (39) still obtains (note that U_0 has dimensions of energy times volume).

Now we consider T such that $\nu > \nu_{\text{crit}}$. In this case a condensate will be present, so we can use eq. (32b) for μ_{nd} . With $U_0 = 0$, $\mu_{\text{nd}} = 0$. As $T \rightarrow 0^+$, the argument of the polylogarithms in eqs. (36) ($\nu > \nu_{\text{crit}}$) and (38) approaches unity, and the functions approach Riemann zeta functions. We now replace the second term in eq. (38) using eq. (36) ($\nu > \nu_{\text{crit}}$). These manipulations yield

$$P = \beta^{-1} (\nu - \nu_0) \frac{\zeta\left(\frac{5}{2}\right)}{\zeta\left(\frac{3}{2}\right)}. \quad (40)$$

Note that this result is what we would obtain if in our eq. (39) (or Tolman's 93.20) we took $\mu_{\text{nd}} = 0$ and replaced ν with $\nu - \nu_0$, which is justified because normally when a condensate appears the chemical potential in the non-degenerate component is set to zero and only the non-degenerate component produces pressure. This is because particles in the condensate have zero momentum down to quantum mechanical uncertainty ($\Delta p_{0, \text{min}} \simeq V^{-1/3} \hbar$) and so should not contribute any pressure.

9 APPENDIX B: DYNAMICAL FRICTION

Goodman (2000) argued that the superfluidity of an RDM condensate implies that there should be no dynamical friction on a moving potential, such as a galactic bar, insofar as the core of the halo is dominated by the condensate and $v_{\text{bar}} < v_{\text{crit}} = \sqrt{2\nu U_0/m}$. Our current view is somewhat different. In the limit that the scattering mean-free-path is large compared to the dimensions of the bar or the core, the original argument is perhaps correct. In the opposite limit, while it remains true that the dynamical friction vanishes below a critical speed $\sim v_{\text{crit}}$, the reason is not because the RDM is a superfluid (although it is), but rather because it is sufficiently ideal fluid in the classical sense, i.e. the viscosity due to collisions between particles and due to the thermal velocity of the particles is negligible.

The important difference between a galactic bar interacting with DM gravitationally and a spoon dragged through a laboratory fluid is that the gravitational potential is smooth, whereas the spoon has a surface at which a no-slip boundary condition applies to the normal (non-superfluid) component. Thus, even in laminar flow, the spoon exerts a viscous force on the normal component that vanishes more slowly than linearly with the viscosity, probably as the Reynolds number $Re^{-1/2}$, because there is a laminar boundary layer. At moderately high Reynolds number, the boundary layer on the rear side of the spoon becomes unstable and contributes a turbulent drag that is asymptotically independent of Re . For a smooth large-scale potential like that of a rotating bar, there is no such surface and no such boundary layer, and therefore perhaps no turbulence. This absence of drag would seem to hold even if the RDM had a substantial normal-fluid component.

However, the bar or other moving potential may experience a wave drag if it couples to a wave whose phase velocity, whether linear or angular, matches that of the potential itself. In a pure condensate, below v_{crit} , the only significant

waves are phonons at speed $c_s = \sqrt{2K\rho}$, so that a linearly moving potential experiences no wave drag if its velocity is subsonic, though a rotating bar could excite phonons at large radii where $|\mathbf{r} \times \boldsymbol{\Omega}_{\text{bar}}| > c_s$. One can see this explicitly from the quantum-mechanical equation of motion for the condensate wave function (Gross-Pitaevskii or non-linear Schrödinger equation):

$$i\hbar \frac{\partial \Psi}{\partial t} = -\frac{\hbar^2}{2m} \nabla^2 \Psi + U_0 |\Psi|^2 \Psi + (\Phi_{\text{self}} + \Phi_{\text{ext}}) \Psi, \quad (41)$$

in which Φ_{ext} & Φ_{self} are the gravitational potentials of the bar or other external perturber and of the condensate itself; Φ_{self} satisfies Poisson's equation with the mass density $\rho_c = m|\Psi|^2$ of the condensate as source.

Adopting the usual Jeans swindle, consider perturbations to a background state of uniform density and vanishing Φ . The unperturbed wavefunction Ψ_0 has a constant modulus $|\Psi_0| = \sqrt{\nu_0}$ but a time-dependent phase, because the term involving U_0 in eq. (41) does not vanish in the background state. One sets $\Psi \rightarrow \Psi_0(t)[1 + \varepsilon(\mathbf{r}, t)]$ and expands eq. (41) to first order in the real and imaginary parts of ε , treating Φ_{ext} and Φ_{self} as well as ε as first-order quantities. In the unforced case $\Phi_{\text{ext}} = 0$, the dispersion relation for Fourier modes $\varepsilon(\vec{r}, t) \propto \exp(i\vec{k} \cdot \vec{r} - i\omega t)$ becomes

$$\omega_k^2 = c_s^2 k^2 - 4\pi G m \nu + \left(\frac{\hbar k^2}{2m}\right)^2, \quad (42)$$

in which $c_s \equiv \sqrt{\nu U_0/m}$ plays the role of sound speed. Chavanis (2011) also obtains this result. As usual with the GP Equation, the last term on the right represents single-particle excitations; it is small for long-wavelength modes $k \ll 2mc_s/\hbar$. If one neglects the term in k^4 , then equation (42) matches the results of a Jeans analysis for a classical ideal fluid, $\omega^2 = c_s^2 k^2 - 4\pi G \rho$ (e.g. Binney & Tremaine 2008).

This conclusion can also be reached if one explicitly computes the drag force on a perturbing body. Consider a rigid perturbing potential that moves at constant velocity v through the condensate, $\Phi_{\text{ext}}(\vec{r} - \vec{v}t)$. If we write $\tilde{\Phi}_{\text{ext}}(\vec{k})$ for the spatial Fourier transform of this potential at any time, then after transients have decayed, the component of the wave drag along \vec{v} is

$$F_{\text{drag}} = -\frac{\rho_0}{V} \int \frac{d\vec{k}}{(2\pi)^3} \delta(\omega_k - \vec{k} \cdot \vec{v}) |\vec{k} \tilde{\Phi}_{\text{ext}}(\vec{k})|^2, \quad (43)$$

with $\rho_0 \equiv m\nu$. Since the Fourier components $\tilde{\Phi}_{\text{ext}}(\vec{k})$ are negligible at $k \gtrsim \sqrt{2mc_s}/\hbar$, this is effectively the same drag as for an ideal fluid with equation of state $P = K\rho^2$. The quantum-mechanical nature of the condensate plays no direct role. To the extent that the self-gravity of the RDM is slight on the scale of the perturber, in other words $\tilde{\Phi}_{\text{ext}}(\vec{k})$ is unimportant for $k^2 \lesssim 4\pi G \rho_0/c_s^2$, the drag vanishes for subsonic motion relative to the condensate.

The formal result (43) holds more generally for ideal fluids in which the dispersion relation may differ from eq. (42). Thus it should hold even when the RDM has a normal (non-degenerate) component, as it must at finite temperature. In a realistic case where the background state is not uniform, however, the RDM gas would be stratified, i.e. it would have an entropy gradient parallel to the background gravitational field, so that waves restored by buoyancy (internal waves/g modes) might be excited at subsonic velocities. As we show

in §3, an isothermal RDM halo at nonzero temperature consists of a core that is almost pure condensate, and has nearly the $n = 1$ Emden profile, surrounded by an extended non-degenerate “atmosphere,” with a sharp cliff in the density profile at the edge of the core (Fig. 2). Although we do not calculate it here, the coupling of a sub-sonically rotating bar potential to the g modes would probably occur mainly just outside the core, with a drag proportional to the density in the non-degenerate component there. Since that density is much less than the central density, the drag on the bar for a given mass-to-light ratio would be much less than what Debattista & Sellwood (2000) estimate for collisionless dark matter. The pattern speeds of their simulated bars slow significantly from their maximum possible values—the values at which corotation with the local galactic circular velocity occurs near the end of the bar—in a few rotation periods.

Typical pattern speeds of galactic bars are measured to be $\Omega_b \lesssim 60 \text{ km s}^{-1} \text{ kpc}^{-1}$, corresponding to rotation periods $2\pi\Omega_b^{-1} \gtrsim 10^8 \text{ yr}$ (Merrifield & Kuijken 1995; Gerssen et al. 1999; Hirota et al. 2009 and references therein). An $n = 1$ Emden polytrope with central sound speed $c_s(0)$, radius r_c , and mass M_c has a circular velocity $v_c \equiv \sqrt{GM_c/r_c} = c_s(0)$. The slowest (fundamental) mode of such a polytrope with the required quadrupolar symmetry ($\ell = m = 2$) has pattern speed $\omega_c/2 = 0.616v_c/r_c$, which is about the same as the measured bar speeds if $v_c = 100 \text{ km s}^{-1}$ and $r_c = 1 \text{ kpc}$. If $\Omega_b < \omega_c/2$, then the bar should not excite this mode, and there should be no torque between the bar and the core. There would probably still be a drag on the surrounding non-degenerate component, but without attempting to calculate this explicitly, we expect by analogy with tidal excitation of g modes in stars (e.g. Goldreich & Nicholson 1989) that the torque on that component would be suppressed by the ratio of the maximum nondegenerate density to the central density of the core, a factor $\sim \theta \ll 1$.